

## MODELING AND VERIFICATION OF MULTI-STRUT MODELING APPROACH OF MASONRY PANEL SURROUNDED BY RC FRAME

Fahim Faisal\*<sup>1</sup>, Md Rayhan Mirza<sup>1</sup>, Sadia Afrin<sup>1</sup> and Debasish Sen<sup>2</sup>

<sup>1</sup> Undergraduate Student, Ahsanullah University of Science & Technology, Bangladesh,

<sup>2</sup> Assistant Professor, Ahsanullah University of Science & Technology, Bangladesh,

Received: 01 December 2021

Accepted: 01 October 2022

### ABSTRACT

Bangladesh which lies in an earthquake-prone region, possesses many seismically vulnerable structures and would need to be strengthened for future usage following the current building code. In this context, assessing the responses of the existing building frames with or without infilled masonry is essential for designing an adequate strengthening scheme that would be suitable for the building. The current study intends to model and simulate one of the available masonry infilled test specimens where the fiber modeling approach of RC member and the multi-strut model of infill masonry have been considered. In addition, the numerically obtained lateral strength has also been compared with analytically evaluated lateral strength. The lateral responses obtained from the numerical analysis showed a fair agreement with the experimental cyclic behavior having a ratio of experimental to the numerical lateral capacity of 0.97. The numerical lateral strength also indicates good conformity with analytical evaluation having an analytical to numerical lateral capacity ratio of 1.13.

**Keywords:** RC frame; Infill masonry; Fiber modeling; Multi strut model; Performance evaluation.

### 1. INTRODUCTION

Masonry infilled RC frame is a widely used structural system around the world. Masonry infill panels have a considerable impact on seismic performance since they've caused severe damage in previous earthquakes (Vielma *et al.*, 2021). It has been found that masonry infill is most commonly used as internal partition walls and exterior walls in buildings depending on its usage. However, they are rarely considered in the numerical analysis since it is challenging to create an appropriate analytical model for infill panels that can simulate the actual behavior. Neglecting the effects of masonry infill can result in an underestimation of structural damage in masonry infilled RC frame structures subjected to cyclic or dynamic loads. But the rigidity and strength of a system are significantly enhanced by using brick infill panels. So, it is important to evaluate the performance of the existing modeling techniques of masonry infilled RC frames through numerical analysis.

The primary objective of this study is to numerically model and investigate the lateral behavior of a bare RC frame and an infill panel surrounded by RC frame that have been experimentally investigated by Seki *et al.* (2018). This paper aims to employ fiber modeling approach for RC frames and multi-strut modeling approach for infill masonry in assessing the lateral performance of the aforementioned test specimens. The second objective is to compare the lateral responses obtained from numerical analysis with experimentally achieved cyclic behavior to validate the utilized numerical models for performance evaluation of the RC frame with infill masonry. In addition, this study also compares the numerically obtained result with the theoretically evaluated lateral capacity of the test specimens for the validation of the numerical model more precisely.

### 2. MODELLING APPROACH

#### 2.1 Reference Test Specimen

The numerical modeling presented in this study represents the experimental tests carried out by Seki *et al.*, (2018) that focus on the retrofit technologies for RC buildings containing masonry walls in developing countries. Five specimens were tested along with a bare RC frame (S1-F) and a masonry infill panel surrounded by RC frame (S3-FM) in that experimental study. Based on their test, the present study intends to simulate the bare RC frame and the masonry infill panel surrounded by RC frame in the SeismoStruct (2021) software.

In Table 1, the material properties of concrete, masonry, and reinforcement have been listed. The dimension and reinforcing steel arrangement of the specimens have been illustrated in Figure 1.

---

\*Corresponding Author: [fahimfaisal7876@gmail.com](mailto:fahimfaisal7876@gmail.com)

<https://www2.kuet.ac.bd/JES/>

ISSN 2075-4914 (print); ISSN 2706-6835 (online)

**Table 1:** Material properties of concrete, masonry, and reinforcement (All values are in MPa)

Specimen	Concrete	Masonry	Reinforcement					
			Φ8		Φ10		Φ12	
	$f'_c$	$f_m$	$f_y$	$f_{ult}$	$f_y$	$f_{ult}$	$f_y$	$f_{ult}$
S1-F	-	-	-	-	-	-	-	-
S3-FM	14	11.6	364	429	454	553	428	525

$f'_c$ = concrete compressive strength,  $f_m$ = masonry compressive strength,  $f_y, f_{ult}$ = yield and ultimate strength of reinforcement.

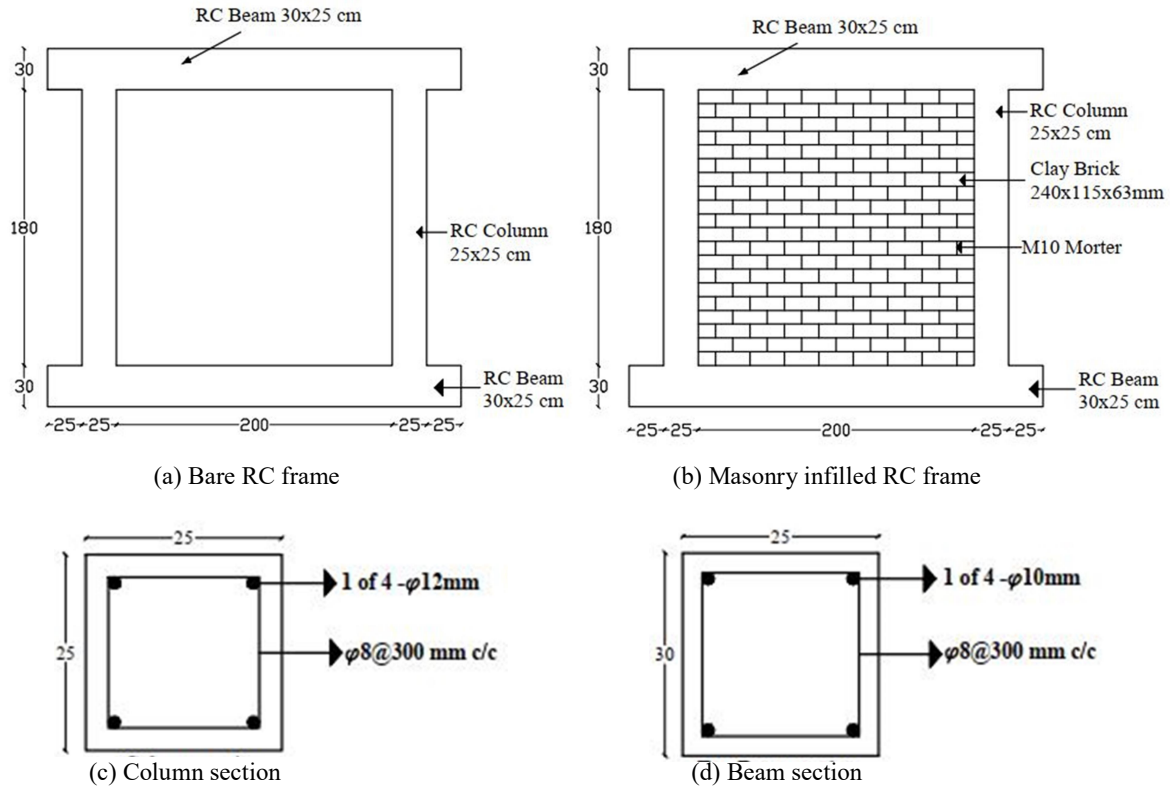


**Figure 1:** Dimension and reinforcement detailing of reference specimens (Dimensions are in cm) (Seki *et al.* 2018).

**2.2 Modelling Scheme**

A finite element software, SeismoStruct (2021), which can predict the substantial amount of deformation behaviors of the RC frames under static or dynamic loading, has been used for this study. The RC frame has been developed using the fiber modeling approach (shown in Figure 2(a)), while the masonry panel has been modeled applying multi-strut model (shown in Figure 3(a)-(b)). At first, column and beam were defined as “infrmDB” element, based on member’s stiffness. This formulation can model space frame members considering geometric and material nonlinearities and can achieve better accuracy for the distribution of deformation (Seismosoft 2021). Each beam and column element has been further subdivided into 300 fibers to obtain better distribution of stress and strains, as shown in Figure 2(b)-(c), considering the nonlinear uniaxial material behavior by integrating the individual fibers. Then a multi-strut model, proposed by Crisafulli & Carr (2007), has been employed for the modeling of infill panels within the bare frame structure. This model is composed of four nodes of masonry panel elements. Each masonry panel consists of four strut members, where two parallel struts in each diagonal direction carry axial loads, and two alternative shear springs transmit the shear from the top to the bottom of the panel in the direction of loading. As shown in Figure 3(a), four internal nodes have been introduced to represent frame and infill contact at the column and beam’s exterior whereas four dummy nodes represent the actual contact length between frame and infill panel. The internal forces have been transferred to the four external nodes where the infill panel is attached to the frame. The axial load struts follow the masonry strut hysteresis model whereas the shear strut follows the bilinear hysteresis rule. Figure 3(b) shows shear modeling using a shear spring in both loading directions.

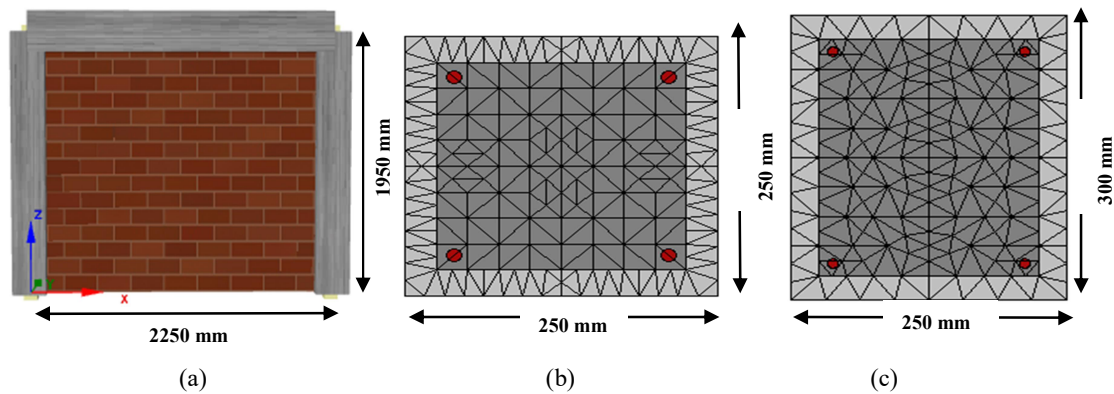


**Figure 2:** (a) Analytical model of masonry infilled RC frame (b) Column section (c) Beam section.

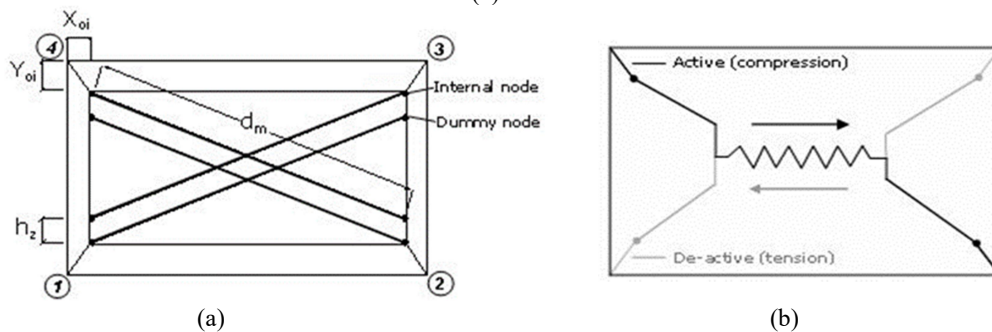


**Figure 3:** (a) Infill panel element configuration (b) Shear spring modelling.

## 2.3 Constitutive Material Models

### 2.3.1 Concrete and Reinforcing Steel Material Models

An in-elastic beam-column element for concrete and reinforcement have been employed for numerical modeling of RC frame members. Specifically, the materials “con-ma” and “stl-gmp” that are available in the SeismoStruct were used for the modeling of concrete and reinforcing steel, respectively. The concrete model “con-ma” is a uniaxial nonlinear model with fixed confinement proposed by Mander *et al.*, (1988). In this model, reinforced concrete members with axial compression forces are confined by transverse steel which enhances the member strength and ductility, creating a fixed effect of confinement and constant confinement pressure has been considered all through the strain-strain range. The Giuffre-Menegotto-Pinto steel model with isotropic hardening (referred to as “stl-gmp”), fully described by Filippou *et al.*, (1983) is a special plasticity model for the cyclic behavior of reinforcing steel. The Giuffre-Menegotto-Pinto (GMP) constitutive stress-strain relationship has been widely utilized to model the nonlinear behavior of steel reinforcement under cyclic loading. Especially when reversal load occurs, this model can be widely used. This model provides a better prediction of stress-strain relation compared to the other formulations available.

### 2.3.2 Cyclic Compression Strut Selation

Crisafulli (1997) proposes a masonry infill strut model which has been used to specify the response of masonry under axial cyclic loads. Six material properties have been used to represent the constitutive rule for the axial cyclic response of the strut as stress-strain relationships, as follows:

(i) Initial modulus of elasticity,  $E_m$ : The elastic modulus, which indicates the primary slope of the stress-strain curve. It has a wide range of values since masonry consists of bricks and mortars. The average value of  $E_m$  which is used here is 550 times  $f_m$ , where  $f_m$ = masonry prism compressive strength, by the proposal by Kaushik *et al.*, (2007).

(ii) Compressive strength,  $f_{m\theta}$ : The compressive strength represents the diagonal capacity of infill panel element which is different from the usual compressive strength of the infill panel. The suitable technique is to compute a strength value for each probable failure mechanism and use the minimum value as compressive

strength. Four different failure mechanisms have been identified by Bertoldi *et al.* (1993). Among these, diagonal tension may not be considered a failure (Moretti 2015), and compression at the corner is similar to diagonal compression failure. It is found in numerous literature that most of the infill panel shows sliding shear failure (Seki *et al.*, 2018, Celano *et al.*, 2021, Zovkic *et al.*, 2012) and compression at the center of the panel (Kaya *et al.*, 2018, Essa *et al.*, 2014, Alwashali *et al.*, 2017). Hence only these two failure mechanisms have been considered herein and the compressive strength ( $f_{m\theta}$ ) corresponding to sliding shear and compression at the center panel is computed as per equation (1) and equation (2), respectively.

$$f_{m\theta} = \frac{(1.2 \sin\theta + 0.45 \cos\theta)f_{wu} + 0.3\sigma_v}{\frac{b_w}{d_w}} \tag{1}$$

$$f_{m\theta} = \frac{1.16 f'_w \tan\theta}{K_1 + K_2 \lambda h} \tag{2}$$

where,  $f_{wu}$ = sliding resistance of mortar joints,  $\sigma_v$ = vertical compressive stress due to gravity loads,  $f'_w$ = fundamental compression resistance,  $d_w$ = diagonal length of the panel,  $b_w$ = effective width of the diagonal strut,  $h$ = infill panel height. The  $K_1$  and  $K_2$  parameters can be expressed as a function of  $\lambda h$ , presented in Table 2, and,  $\lambda$  is a dimensionless relative stiffness parameter, expressed as equation (3).

$$\lambda = \sqrt[4]{\frac{E_m t_m \sin 2\theta}{4 E_c I_c h_w}} \tag{3}$$

where,  $E_m$ = elastic modulus of the masonry,  $t_m$ = infill panel thickness,  $E_c$ = elastic modulus of concrete,  $\theta$ = angle of diagonal with horizontal and  $I_c$ = moment of inertia of column and  $h_w$ = infill panel height.

**Table 2:** The Parameters of K1 and K2 (Skafida *et al.*, 2014).

	$\lambda h < 3.14$	$3.14 < \lambda h < 7.85$	$\lambda h > 7.85$
<b>K<sub>1</sub></b>	1.3	0.707	0.47
<b>K<sub>2</sub></b>	-0.178	0.010	0.04

(iii) Tensile Strength,  $f_t$ : It specifies the masonry’s tensile strength or the bond strength of the contact between frame and infill panel. It is assumed to be zero as it has a lower value compared with compressive strength and has a negligible impact on the total behavior.

(iv) Strain at maximum stress,  $\epsilon_m$ : It specifies the strain at maximum stress and is influenced by changes in the secant stiffness of the stress-strain curve’s ascending branch.

(v) Ultimate strain,  $\epsilon_{ult}$ : It regulates the stress-strain curve’s descending branch, which is developed using a parabola to ensure strut response is as controlled as possible.

(vi) Closing strain,  $\epsilon_{cl}$ : It specifies the strain when the cracks are slightly closed allowing compressive stress to form.

Furthermore, Crisafulli (1997) proposes a set of empirical parameters based on the results of experiments associated exclusively with the cyclic behavior to fully define the hysteretic behavior of the masonry panel as shown in Table 3.

**2.3.3 Cyclic Shear Spring Relation**

Crisafulli (1997) proposes a bilinear model that represents the cyclic behavior of the shear spring. The shear strength of the infill panel can be expressed as a combination of two mechanisms named resistance to friction between bricks and mortar joints and bond strength. Four parameters were defined hereinafter, namely the friction coefficient, maximum shear strength, shear bond strength, and reduction shear factor, to fully characterize the shear cyclic relationship in the model.

**2.3.4 Geometric Properties of The Masonry Panel**

The geometric properties as stated below are needed to fully define the masonry panel model.

(i) Thickness of infill panel: It can be expressed as equal to the panel bricks width alone or including plaster contribution, which is 115 mm in this study.

(ii) Initial and reduced strut area: The initial strut area of the masonry panel is a product of the equivalent width of the strut and the panel thickness. The expression proposed by Klingner & Bertero (1978) has been used to compute the equivalent strut width. The reduced strut area is represented as a percentage of the initial strut area. A higher value (e.g. 95%) of the initial strut area gives smooth degradation of stiffness while lower value (e.g.

10%) gives sudden degradation. The initial strut area of the specimen is found to be 30795 mm<sup>2</sup> and 95% of initial strut area has been used as the reduced strut area in this study.

(iii) Equivalent contact length: It represents the vertical height of the panel in percentage, which provides the distance between dummy nodes and internal nodes. In this study, 13% of vertical height of the panel has been used as equivalent contact length.

(iv) Horizontal and Vertical offsets: They represent the distance between exterior corner nodes and internal nodes. Horizontal offset is the percentage of the ratio of column depth and masonry length and vertical offset is the percentage of the ratio of beam depth and masonry height and the values are 12.50% and 16.67%, respectively for this study.

(v) Proportion of stiffness assigned to shear: It represents proportion to the panel stiffness to which shear springs should be allocated, which is considered 5% in this study.

The parameters used for the diagonal strut and shear spring of the masonry panel are presented in Table 3.

## 2.4 Load and Restraint

The models have been subjected to cyclic lateral loading and a continuous axial load of 350 kN has been applied on each column which is similar to the experimental loading protocol. The cyclic lateral loading was consisted of two cycles for each lateral drift of 0.0625%, 0.125%, 0.25%, 0.50%, 1.0%, 1.5%, 2.0% and 3.0%. All nodes at the base of the columns have been restrained in all directions to prevent any rotation and translation.

**Table 3:** Simulated parameters of the strut and shear spring element of the specimen.

Parameters	Unit	Value
Initial modulus of elasticity, $E_m$	MPa	6380
Compressive strength of masonry panel, $f_{m\theta}$	MPa	1.25
Tensile strength of masonry panel, $f_t$	MPa	0
Strain at maximum compressive stress, $\varepsilon_m$	-	0.0036
Closing strain, $\varepsilon_{cl}$	-	0.003
Ultimate strain, $\varepsilon_{ult}$	-	0.072
Shear bond strength of masonry panel, $\tau_o$	MPa	0.35
Friction coefficient, $\mu$	-	0.70
Maximum shear stress, $\tau_{max}$	MPa	0.65
Shear reduction factor, $\alpha_s$	-	2
Starting unloading stiffness factor, $\gamma_u$	-	1.5
Strain inflection factor, $\alpha_{ch}$	-	0.6
Strain reloading factor, $\alpha_r$	-	0.4
Stress inflection factor, $\beta_{ch}$	-	0.7
Complete unloading factor, $\beta_a$	-	2.0
Reloading stiffness factor, $\gamma_{ptr}$	-	1.25
Zero stress stiffness factor, $\gamma_{ptu}$	-	1.0
Plastic unloading stiffness factor, $e_{x1}$	-	2.0
Repeated cycle strain factor, $e_{x2}$	-	1.5

## 3. STRENGTH EVALUATION OF RC FRAME AND MASONRY INFILLED RC FRAME

### 3.1 Strength Evaluation of Bare RC Frame

The lateral resistance of bare RC frame has been evaluated considering the minimum lateral strength of RC columns considering both shear hinge at middle and flexural hinges at top and bottom of the column. The lateral capacity of RC frame ( $Q_{fr}$ ) has been calculated as per JBDPA (2001), using equation (4), (5), (6), (7).

$$Q_{fr} = 2 * \min[Q_{su} \& Q_{mu}] \quad (4)$$

Where,  $Q_{fr}$  = bare RC frame capacity,  $Q_{su}$  = shear strength of RC frame and  $Q_{mu}$  = ultimate flexural strength of RC frame.

The ultimate shear strength of column has been computed using equation (4). The ultimate shear strength of beam has been ignored here because beam hardly fails under shear.

$$Q_{su} = \left( \frac{0.053 p_t^{0.053} * (18 + F_c)}{M/Q + 0.12} + 0.85 \sqrt{p_w * \sigma_{wy}} + 0.1 \sigma_o \right) * b * j \quad (5)$$

where,  $p_t$ = ratio of tensile rebar (%),  $p_w$ = ratio of shear rebar,  $\sigma_{wy}$ = yield strength of shear rebar,  $\sigma_o$ = axial stress in column,  $M/Q$ = length of shear span ( $h_o/2$  is default value),  $d$ = effective depth of column,  $j$ = distance between centroid of compression and tension force.

The flexural strength of the frame ( $Q_{mu}$ ) has been computed from equation (6) considering the moment capacity of RC columns ( $M_u$ ) as well as beam ( $M_b$ ). As per equation (7), the ultimate moment capacity of the column has been calculated considering the effect of axial loads. The ultimate moment capacity of beam has been calculated from equation (8).

$$Q_{mu} = \frac{M_u + \text{Min}(M_u \& M_b)}{h} \quad (6)$$

$$M_u = (0.8 a_t * \sigma_y * D + 0.12 b * D^2 * F_c) * \left( \frac{N_{max} - N}{N_{max} - 0.4 b * D * F_c} \right) \quad (7)$$

$$M_b = 0.9 a_t * \sigma_y * d \quad (8)$$

where,  $N$ = Axial force,  $N_{max}$ = axial compressive strength =  $b x D x F_c + a_g x \sigma_y$ ,  $N_{min}$ = Axial tensile strength =  $-a_g x \sigma_y$ ,  $a_t$ = total cross sectional area of tensile reinforcement ( $\text{mm}^2$ ),  $a_g$ = total cross sectional area of reinforcement ( $\text{mm}^2$ ),  $b$ = column width,  $D$ = column depth,  $\sigma_y$ = yield strength of reinforcement,  $F_c$ = concrete compressive strength,  $d$ = effective depth of beam.

### 3.2 Strength Evaluation of Masonry Infilled RC Frame

The lateral resistance of the infill panel surrounded by RC frame ( $Q_{mas}$ ) has been evaluated as the summation of infill masonry capacity and frame capacity considering minimum of diagonal compression ( $Q_{mas,comp}$ ) and sliding capacities ( $Q_{mas,sliding}$ ).

In case of diagonal crushing failure, a diagonal strut forms and crushes inside the RC frame eventually. The strut width has been computed using equation (9), (10) as proposed by Mainstone (1971), which is also suggested by FEMA 306. The lateral capacity of infill during crushing is considered as the horizontal component of diagonal strut capacity as equation (11).

$$a = 0.175 * (\lambda * h_{col})^{-0.4} * r_{inf} \quad (9)$$

$$\lambda = \left( \frac{E_m * t_{inf} * \sin 2\theta}{4 E_f * I_{col} * h_{inf}} \right)^{0.25} \quad (10)$$

$$Q_{mas,comp} = a * t_{inf} * f_{m90} * \cos \theta \quad (11)$$

and,  $a$ = equivalent strut width,  $\lambda$ = stiffness parameter,  $h_{col}$ = column height at centerlines of beam,  $I_{col}$ = moment of inertia of column,  $h_{inf}$ = height of masonry infill,  $t_{inf}$ = thickness of infill,  $E_f$ = modulus of elasticity of frame material,  $E_m$ = modulus of elasticity of the infill material,  $\theta$ = angle between diagonal and horizontal and  $r_{inf}$ = diagonal length of masonry infill,  $f_{m90}$ = masonry compressive strength at horizontal direction ( $=0.5 f_m$  as proposed by FEMA 306),  $f_m$ = masonry compressive strength.

And, the lateral capacity of infill during sliding has been calculated as using equation (12) as per Paulay & Priestly (1992).

$$Q_{mas,sliding} = \left[ \left( \frac{0.03 m}{1 - \mu * \frac{m}{L_{inf}}} \right) * L_{inf} * t_{inf} \right] \quad (12)$$

Where,  $\mu$ = Co-efficient of friction= 0.45,  $L_{inf}$ = Length of infill panel.

## 4. VERIFICATION OF THE NUMERICAL MODEL

The numerically obtained lateral behaviors of the bare RC frame and infill panel surrounded by RC frame have been compared with the experimentally achieved cyclic behavior as well as the theoretically obtained lateral strength.

#### 4.1 Experimental Result

The bare frame exhibited the highest lateral resistance of 81 kN and -79 kN at 1.0% and -1.5% story drift, respectively. The specimen failed at 2% story drift in the negative cycle by flexural hinge formation at bottom and top of the column. Adding of the masonry wall significantly enhanced the lateral resistance to 156 kN and -191 kN at 1.0% and -1.0% story drift, respectively, which is 2.2 times greater than the bare frame capacity and the specimen failed at 3% story drift. The full details of lateral cyclic behavior of can be found in Seki *et al.*, (2018).

#### 4.2 Analytical Result

The theoretically computed capacities of bare frame and masonry infilled RC frames have been presented in Table 4. The lateral capacity of the bare RC frame was found to be 68.20 kN, shows good agreement with experimental capacity of 80 kN (average of both directions), with a ratio of experimental to analytical capacity of 1.17.

For infill panel surrounded by RC frame, the lateral capacity of the surrounding frame and the bare frame has been considered equal. As discussed in earlier section, the capacity of infill panel is minimum of sliding capacity and diagonal compression capacity, but in this study both the capacities has been found almost equal. The calculated lateral capacity of 202.95 kN shows fair agreement with experimental capacity of 173.5 kN (average of both directions), with a ratio of experimental to analytical capacity of 0.85.

**Table 4:** Analytical capacity of the specimens.

Specimen	$M_u$	$M_b$	$Q_{mu}$	$Q_{su}$	Frame Capacity	$Q_{mas(comp)}$	$Q_{mas(sliding)}$	Masonry Infilled RC Frame Capacity (kN)
	(kN)	(kN)	(kN)	(kN)	(kN)	(kN)	(kN)	(kN)
Bare RC Frame (S1-F)	45.61	16.36	34.42	79.20	68.84	-	-	-
Masonry infilled RC frame (S3-FM)	45.61	16.36	34.42	79.20	68.84	134.11	134.52	202.95

#### 4.3 Comparison With Numerical Result

The bare frame showed maximum lateral resistance of 68 kN and 91 kN at 0.5% and -1.5% story drift, respectively while the masonry infilled RC frame showed maximum lateral resistance of 160 kN and 197 kN at 0.5% and -0.5% story drift, respectively after simulating the models in the software.

Figure 4 represents the comparison between numerical and experimental results of the specimens in terms of lateral load resisting capacity. For bare frame, Figure 4(a) shows that experimental and numerical result agrees well regarding initial stiffness however, a significant deviation of stiffness has occurred in inelastic stage. The numerical model underestimates the peak strength in positive direction and overestimates in negative direction in comparison to experimental result having a ratio of experimental to numerical capacity of 1.0 (average of both directions). The graph also explains that the peak strength achieved at same story drift (-1.5%) in negative drift cycle but at different story drift in positive drift cycle. After reaching peak strength, sudden degradation can be observed in experimental result while the numerical result shows gradual degradation in terms of lateral resistance.

For infill panel surrounded by RC frame, Figure 4(b) shows that the initial stiffness obtained from the numerical analysis shows good conformity with experimental result while the stiffness at inelastic stages deviates. The peak strength predicted by the numerical model in both directions also shows good agreement with experiment but the peak strength achieved at different story drift in both directions. After reaching peak strength, smooth degradation can be noticed in both experimental and numerical results in terms of lateral resistance.

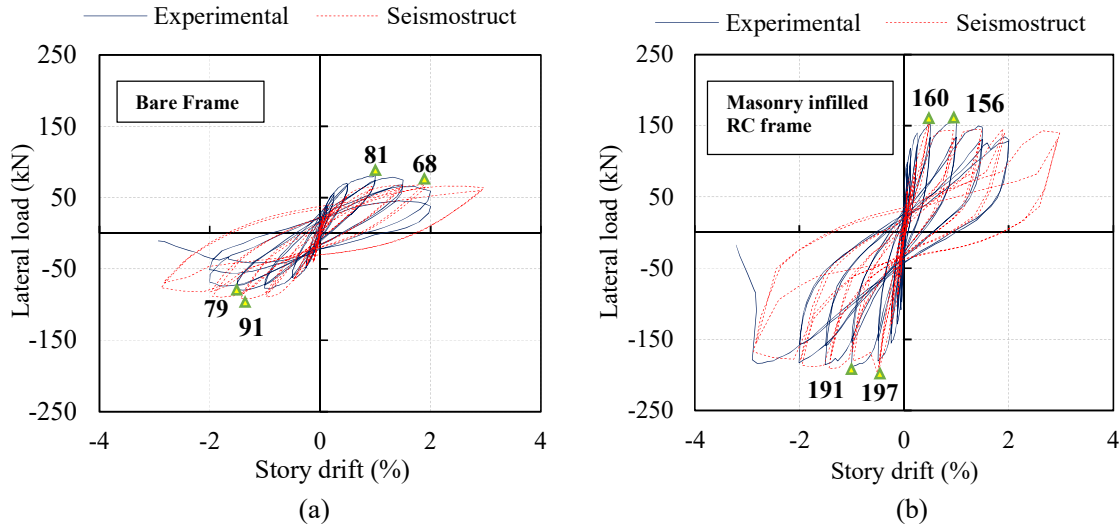


**Figure 4:** Comparison graph of numerical and experimental results of (a) Bare RC frame (b) Masonry infilled RC frame.

The theoretically evaluated lateral capacity of the bare RC frame of 68.20 kN, shows good agreement with numerically obtained capacity (average of both directions), with a ratio of analytical to numerical capacity of 0.86. For masonry infilled RC frame, the calculated lateral capacity of 202.95 kN shows fair agreement with numerical results (average of both directions), with a ratio of analytical to numerical capacity of 1.13. Therefore, the utilized lateral behavior evaluation procedure for both the specimens can precisely predict the actual lateral behavior of masonry infill panel surrounded by RC frame.

Table 5 shows comparison of the numerically evaluated lateral resistance of the specimens with experimental result as well as with analytical evaluation.

**Table 5:** Comparison of Lateral resistance of all the specimens.

Specimen	Lateral resistance								
	Experimental (kN)			Numerical (kN)			$Q_e/Q_n$	Analytical (kN)	
	Positive	Negative	Avg.	Positive	Negative	Avg.		$Q_e/Q_n$	$Q_t/Q_n$
Bare RC frame	81	79	80	68.20	91.87	80.04	1	68.84	0.86
Masonry infilled RC frame	156	191	173.5	160.29	197.41	178.85	0.97	202.95	1.13

**5. CONCLUSION**

This study presents numerical modeling and simulation of one bare frame and one masonry infilled RC frame in SeismoStruct software based on one of the available experimental tests by Seki *et al.*, (2018). The numerically obtained lateral behaviour of the aforementioned test specimens have been validated by comparing the simulated results with experimental ones, also with theoretically evaluated lateral strength. The lateral responses of both the specimens obtained from numerical analysis showed a fair agreement with the experimental cyclic behavior having a ratio of experimental to numerical lateral capacity of 1.0 and 0.97, respectively. The numerical lateral strength of both the specimens also indicates good conformity with analytical evaluation having analytical to numerical lateral capacity ratio of 0.86 and 1.13, respectively. Therefore, the utilized approach of numerical modelling by SeismoStruct is capable of simulating the actual structural behavior of RC frames with and without infilled masonry for seismic performance evaluation if all the parameters are given accurately.

## 6. REFERENCES

- Alwashali, H., Torihata, Y., Jin, K., & Maeda, M. (2018). Experimental observations on the in-plane behaviour of masonry wall infilled RC frames; focusing on deformation limits and backbone curve. *Bulletin of Earthquake Engineering*, 16(3), 1373-1397.
- Bertoldi, S., Decanini, L., Santini, S., & Via, G. (n.d.). Analytical models of infilled frames. *10th European Conference on Earthquake Engineering*. Vienna, Austria.
- Celano, T., Argiento, L. U., Ceroni, F., & Casapulla, C. (2021). Literature Review of the In-Plane Behavior of masonry walls: Theoretical vs. Experimental results. *Materials*, 14(11), 3063.
- Crisafulli, F. J. (1997). *Seismic Behaviour of Reinforced Concrete Structures with Masonry Infills*. PhD Thesis, University of Canterbury, New Zealand.
- Crisafulli, F. J., & Carr, A. J. (2007). Proposed macro-model for the analysis of infilled frame structures. *Bulletin of the New Zealand Society for Earthquake Engineering*, 40(2), 69-77.
- Basic procedures manual (1998): Evaluation of earthquake damaged concrete and masonry wall buildings. *Federal Emergency Management Agency, FEMA 306*.
- Filippou, F.C., Popov, E.V., & Bertero, V.V. (1983). *Effects of bond deterioration on hysteretic behaviour of reinforced concrete joints*. Earthquake Engineering Research Center, University of California.
- Kaushik, H. B., Rai, D. C., & Jain, S. K. (2007). Stress-Strain Characteristics of Clay Brick Masonry under Uniaxial Compression. *Journal of Materials in Civil Engineering*, 19(9), 728-739.
- Kaya, F., Tekeli, H., & Anil, Ö. (2018). Experimental behavior of strengthening of masonry infilled reinforced concrete frames by adding rebar-reinforced stucco. *Structural Concrete*, 19(6), 1792-1805.
- Klingner, R. E., & Bertero, V. V. (1978). Earthquake Resistance of Infilled Frames. *Journal of the Structural Division*, 104(6), 973-989.
- Mainstone, R. J. (1971). On the stiffnesses and strengths of infilled frames. *Proc. of the Institution of Civil Engineers*, 49(2), 230.
- Mander, J. B., Priestley, M. J., & Park, R. (1988). Theoretical Stress-Strain Model for Confined Concrete. *Journal of Structural Engineering*, 114(8), 1804-1826.
- Moretti, M. L. (2015). Seismic design of masonry and reinforced concrete infilled frames: a comprehensive overview. *American Journal of Engineering and Applied Sciences*, 8(4), 748.
- Paulay, T., & Priestly, M. J. (1992). *Seismic design of reinforced concrete and masonry buildings*. Wiley, New York.
- SeismoSoft 2021. SeismoStruct user manual. [https://seismosoft.com/wpcontent/uploads/prods/lib/SeismoStruct-2021-User-Manual\\_ENG.pdf](https://seismosoft.com/wpcontent/uploads/prods/lib/SeismoStruct-2021-User-Manual_ENG.pdf)
- Seki, M., Popa, V., Lozinca, E., Dutu, A., & Papurcu, A. (2018). Experimental study on retrofit technologies for RC frames with infilled brick masonry walls in developing countries. *Proceedings of the 16th ECEE, Greece*.
- Skafida, S., Koutas, L., & Bousias, S. N. (2014). Analytical modeling of masonry infilled RC frames and verification with experimental data. *Journal of Structures*, Article ID: 216549.
- Standard for seismic evaluation of existing concrete buildings. (2001). Japan Building Disaster Prevention Association.
- Tawfik Essa, A. S. A., Kotb Badr, M. R., & El-Zanaty, A. H. (2014). Effect of infill wall on the ductility and behavior of high strength reinforced concrete frames. *HBRC Journal*, 10(3), 258-264.
- Vielma, J. C., Aguiar, R., Frau, C., & Zambrano, A. (2021). Irregularity of the distribution of masonry infill panels and its effect on the seismic collapse of reinforced concrete buildings. *Applied Sciences*, 11(18), 8691.
- Zovkic, J., Sigmund, V., & Guljas, I. (2013). Cyclic testing of a single bay reinforced concrete frames with various types of masonry infill. *Earthquake engineering & structural dynamics*, 42(8), 1131-1149.